P1-18 Effect of Obstruction at Telescope on Geometrical Form Factor in Lidar

Toshiyuki Murayama, Naseru Hagiwara and Shigekazu Sakida
Physics Department, Tokyo University of Mercantile Marine
2-1-6 Etchujima, Koto-ku, Tokyo 135-8533, Japan
Phone: (03)5245-7464, FAX: (03)5245-7339, E-mail: murayama@ipc.tosho-u.ac.jp

1. Introduction

Adaptation and/or evaluation of the geometrical form factor in lidar, so–called overlapping function *Y(R)*, become necessary according to the requirement of observation, especially when we want to retrieve the near-field lidar signals. In our lidar measurements in the boundary layer, we used alternative or two field of view (FOV), i.e., a narrow (1 mrad in full width) and a wide (3-6 mrad) FOV, telescopes to cover the wide dynamic range (Murayama et al., 1996, 1998). We also took into account of the position of the interference filter in receiving optics to reduce the change of the transmission of the collected light with range, keeping the optics as short as possible (Murayama, 1996). Thus we could approximately describe the behavior of the near-field signal by the theoretical calculation based on the geometrical optics (Halldórsson and Langerholc, 1978, Harms, 1979, Measure, 1984).

Here we will describe the effect of the obstructions in the Schmidt-Cassegrain telescope and present a new application of the obstruction for the evaluation of the overlapping function.

2. Effect of the secondary mirror in *Y(R)*

Schmidt-Cassegrain telescope is widely used for lidar application owing to its compactness, which has a central obstruction, i.e., the secondary mirror at the correcting plate. This obstruction cause a dip in the near-field lidar signal in some cases (Murayama, 1994). It is well explained as a result of the insertion process of the shadowing confusion of the secondary mirror at the field stop as shown in Figure 1. One of the most striking dips is appeared when the distance between the axis of the laser beam and the one of the telescope is short and the telescope is inclined toward the laser beam. Such an example is shown with numerical simulations in Figure 2. Thus the numerical simulation fairy well reproduced the feature of the *Y(R)* so as to design and predict the *Y(R)* for the specific optical arrangement.

3. Application of the obstruction to evaluate *Y(R)*

When we do the measurement including Raman channel, we need much higher pulse energy of the emitting laser than we do Mie lidar observation only. In our present system, we use two receiving telescopes for Mie-polarization channels and another for Raman channels (Murayama, 1998). Therefore for Mie-Raman observation case, we have to reduce the receiving light powers for Mie-channel detectors (photomultiplier tubes: PMT) by neutral density filter or decreasing the applying voltages to PMTs to avoid the saturation of the signals. In place of doing so, we found that a versatile method, which is applicable to obtain a more rapid-rising *Y(R)* at the same time. That is, we put the circular cover, which is partly cut out as fan-shape from the center with a certain angle to reduce the backscattered light. For example, when we increased the laser power from 20 mJ to 100 mJ (5 times) and put the 72-degree fan-shape cut plate over the correcting plate, the amount of the receiving light power is same in both cases. Then we have no need to adjust the sensitivities of Mie-channel PMTs. At the same time, we can easily control the overlapping function by choosing the direction of cut area relative to laser beam position. A schematic image of the confusion due to this obstruction whose cut area is set toward the laser beam by dashed lines in Figure. 1. An example of measurements with and without the obstruction in this position is shown in Figure 3. It is clearly seen that the *Y(R)* in the case with the obstruction rise rapidly than the case without it. The *Y(R)* due to obstructed telescope varies significantly with the position of fan-shaped aperture. We will present the numerical simulation of *Y(R)* in these cases.

4. Summary

The numerical calculation of the overlapping function works well when we can disregard the change of the transmission of the interference filter with range. It is useful to simulate the behavior of *Y(R)*. An additional obstruction can give a rapid-rising *Y(R)* than the *Y(R)* without it. This simple method is applicable to evaluate the overlapping function without the obstruction when we made the measurements with and without it during a short time.

References

Halldórsson, T. and Langerholc, J. (1978), Geometrical form factors for the lidar function. *Applied Optics*, 17(12):240-244.

Harms, J. (1979), Lidar return signals for coaxial and noncoaxial systems with central obstruction. *Applied Optics*, 18(10):1559-1566.

Measure, R. M. (1984), *Laser Remote Sensing* (John Wiley & Sons) Chapter 7.

Murayama, T. (1994), Lidar observation of the troposphere in Tokyo. *Abstract of Papers in 17th International Laser Radar Conference,* Sendai, Japan: 66-67.

Murayama, T., Furushima, M., Oda, A., Iwasaka, N., and Kai, K. (1996), Depolarization Ratio Measurements in the Atmospheric Boundary Layer by Lidar in Tokyo. J. Meteorol. Soc. Japan, 74(4):571-578.

Murayama, T., Kaneyasu, N., Kamataki, H., Otsuka, S., Furihata, M., Iwasaka, N., and Tsukamoto, T. (1998), Monitoring of the atmospheric boundary layer with lidar, sun-photometer and filter-sampling in Tokyo. *Proc. of SPIE*, 3504:16-25.

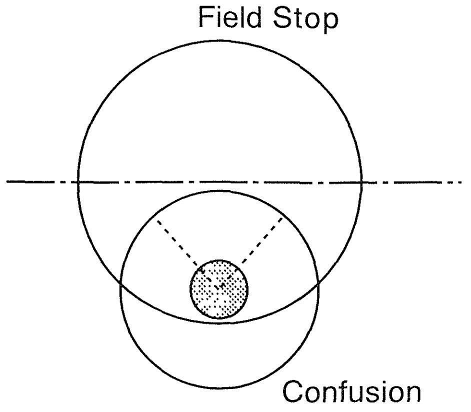

Figure 1. Schematic images of confusion at the field stop from a near-field range. The shaded circle represents the shadowing confusion by the secondary mirror.

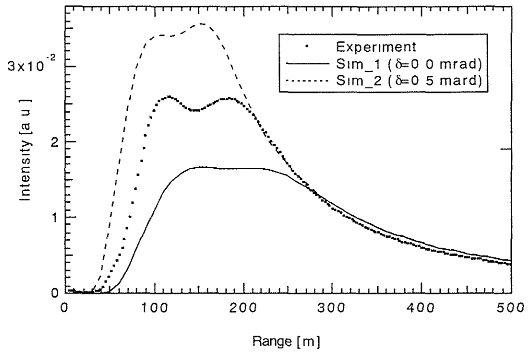

Figure 2. Lidar return signal and the simulations. Followings are system parameters: diameter of telescope=20 cm, distance between the laser beam and the optical axis = 16.5 cm, FOV of telescope =2 mrad, beam divergence=0.16 mrad. δ represents the inclination angle of the telescope axis to the laser beam.

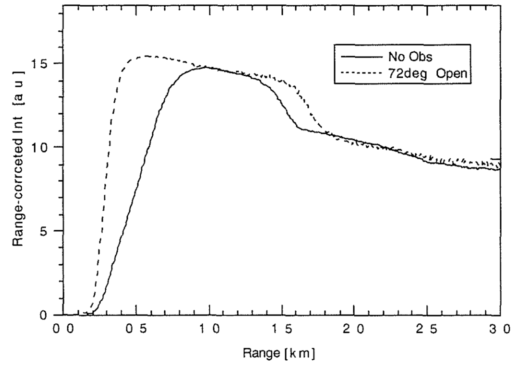

Figure 3. Range corrected lidar return signals with and without the obstruction. The vertical scale is adjusted so as to superpose.